Winding Type Alternation of a Refurbished Old Generator

Nail Tosun*,‡, Görkem Gülletutan*, Muhammet Samet Yakut*, Deniz Alp Yilmaz†, Özgür Bayer†, and Ozan Keysan*,§
* Department of Electrical and Electronics Engineering, Middle East Technical University
† Department of Mechanical Engineering, Middle East Technical University
‡ Electrical Power Group, Newcastle University, Newcastle upon Tyne, NE1 7UR United Kingdom
§ corresponding author: keysan@metu.edu.tr

***Abstract*—Refurbishment of hydro-generators promises an increased lifespan and improved efficiency. Old generators are not only less efficient but also less reliable; their fault occurrence is more common. The economic impact of out-service time can be astronomical. Thus, refurbishment is a critical task; but it is challenging too. Most of the conducted works focus on the material update, enhancing the cooling network, and obtaining better efficiencies. Modifying winding type, i.e. conversion from lap winding to wave winding is rare since it often requires a change in the slot number. Such a move can be laborious, size change can become mandatory. In this study, a refurbishment design strategy is proposed which includes a winding type conversion. The task is to implement a wave winding since it has less out-service time and is easily replaced by field workers. In this paper, an old generator that started operation in 1956 is used for a refurbishment. This study promises a guideline to hydro-generator designers who work on a refurbishment study on old hydro-generators that have diamond coils.**

***Index Terms*—Hydroelectric generators; power generation; rotating machines; synchronous generators.**

I. Introduction

Hydropower installations in many developed countries date back to waves of major construction from the 1960s to the 1980s. 40% of the hydropower plants are at least 40 years old (with an average of 32) which results in 430 GW installed power. These generators have reached their first lifespan; refurbishment is the easiest and cheapest way to increase their operation time without creating any environmental damage. Thus, maximizing the performance, life-span, even maybe output power (in the case of uprating) is the best way to utilize hydropower for mankind.

The interested generator is designed by Westinghouse Electric Corporation and operates for more than 60 years. It is 44444 kVA, 13.8 kV, and 32 poles salient pole synchronous machine. The nameplate of the interested generator is shown in Fig. 1.

Refurbishment projects can promise high-profit returns to the economy. In Fig. 2, hydro-power stations in Turkey are illustrated regarding their commission data and installed power. Considering the total 24.35 GW installed power, generators which have 60+ age contribute 2%, and generators that have 40+ age grant 12.4%. These contributions are also listed in Table I. The hydro generator half-life may be achieved within

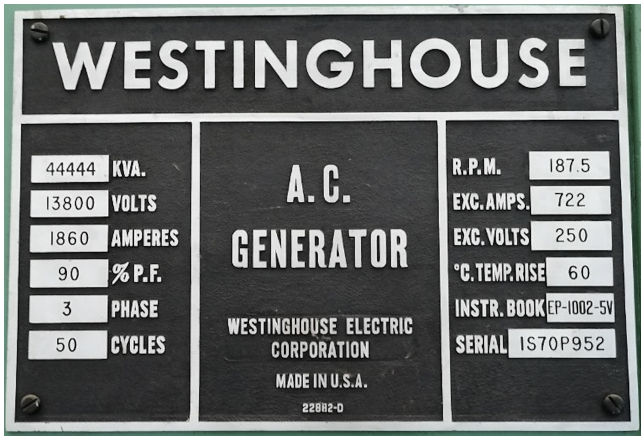

Fig. 1. The name plate of the existing generator.

30 to 60 years of operation, based on the original design's resilience and the harshness of its operational life [1]. This means nearly 30% of the hydro-generators have the potential to be upgraded. Academics are also interested in the refurbishing because it could involve a challenging design problems. The majority of the publishing efforts made by Znidarich; these studies are based on core replacement [2], [3], and stator winding renovation [4]–[7]. In this article, a winding type alternation is proposed in addition to the current literature. An industrial partner has received a specific complaint regarding diamond-type windings, so all new designs are restricted to Roebel windings only. Contrary to Roebel bars, which are

TABLE I
Age Distribution of Old Hydro-generators Connected to the Turkish Grid.

Age	Number of Plants	Capacity (MW)	Contribution[1]
60+	5	493	2%
50-60	3	399	1.6%
40-50	6	2129	8.7%
30-40	9	3894	19.6%

[1] The dividend is total installed capacity of hydro-power plants which have more than 50 MW capacity (24.35 GW).

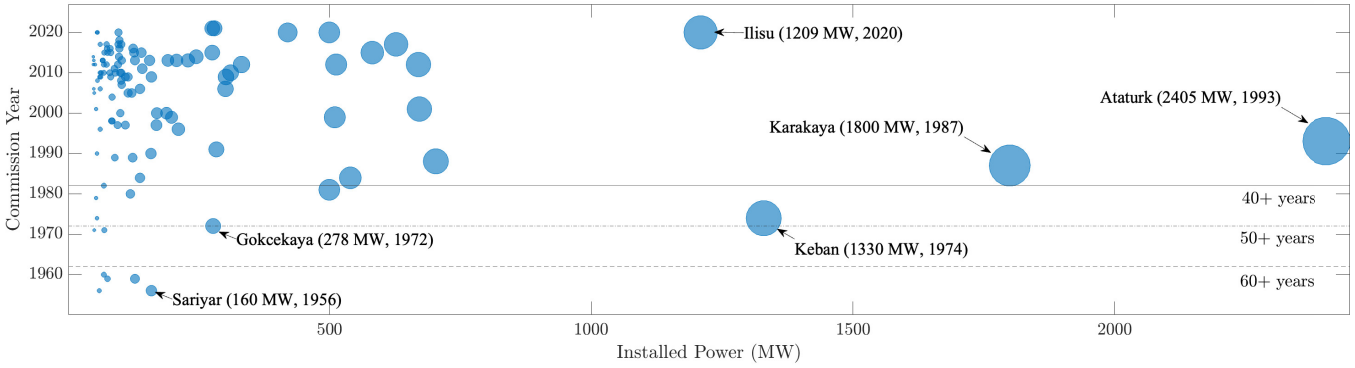

Fig. 2. Hydro-power station installations over years in Turkey. Both the horizantal axis and the size of the bubbles represent the installed power. Lateral lines indicate the age of the generators. The interested generator is located in Sariyar HES(4x40 MW). The top three largest hydro-power stations, Ataturk HES, Karakaya HES, and Keban HES are also indicated in the graph.

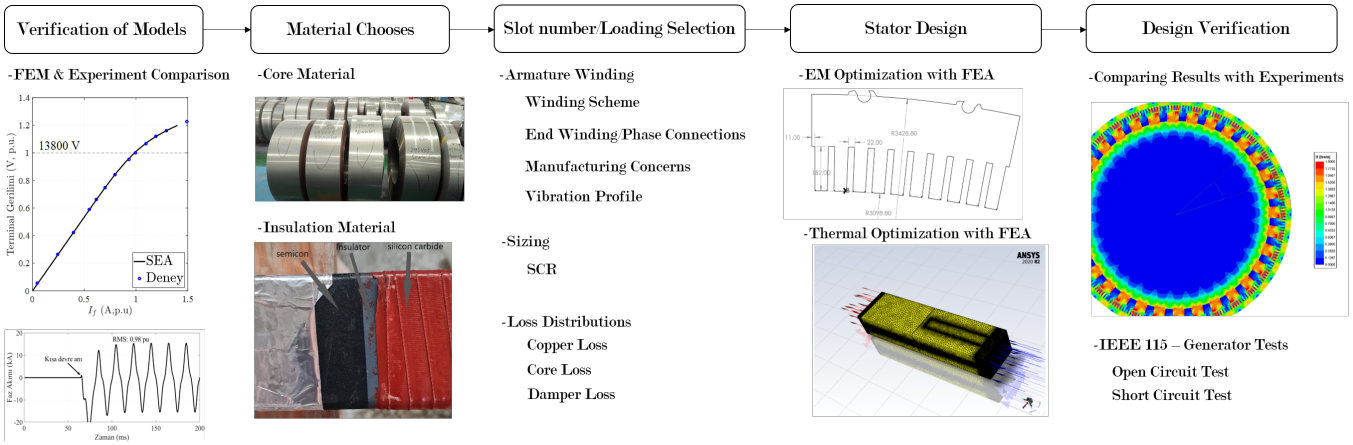

Fig. 3. The refurbishment methodology.

simpler to replace, the out-of-service time is a significant disadvantage for diamond type windings. One of these diamond coils failed in 2002, due to a strand short circuit that required 21 days of operation (with a cost of 19.14 GWh, which result in $\approx$ 3.47 M€). Thus, this study offers a design methodology for hydro-generators with a special emphasis on winding-type alternation.

II. Refurbishing Methodology

The strategy which we used for the refurbishment project is outlined in detail in this section. This is illustrated in Fig. 3. In the following subsections, each step is explained in detail.

A. Validation of Simulation Model

Open-circuit tests are made based on IEEE 115 standard [8], and it is used to validate both analytical and FEA models. Moreover, the original open circuit curve that is obtained after the initial installation (1956) is also considered. This is mainly due to the discrepancy between field tests, and data-sheet values. Akiror *et. al.* [9] also mentioned such issue. Although these generators share the same nameplate and design, the open-circuit curves are considerably different, notably in the saturation zone. Thus, the authors suggest redoing the machine tests.

The open circuit tests are illustrated in Fig. 4. GEN3 and GEN4 are the code names for existing generators; both shares the same nameplate. The black line indicates the curve obtained in 1956. Open circuit curves are obtained this year (2022) also; these curves are illustrated with blue and red lines. Vertical error bars indicated 5% error margins. All three experimental results are different in a noticeable manner.

The design of the electrical machines heavily depends on the accuracy of the models. To avoid the aforementioned concerns, a recently commissioned hydro-generator is used to validate the models. In Fig. 5.a, the comparison of the experiment and simulation is shown, whereas a similar result for the GEN3 is illustrated in Fig. 5.b.

B. Material Chooses

1) Core Materials: Hydro generator stator cores are constructed from laminated electrical steels that are low loss, non-grain oriented, and have a silicon content of 2.8-3.4% [2]. By changing only the core material, the same author was able to reduce the core loss of a 50 MVA hydro generator from 290

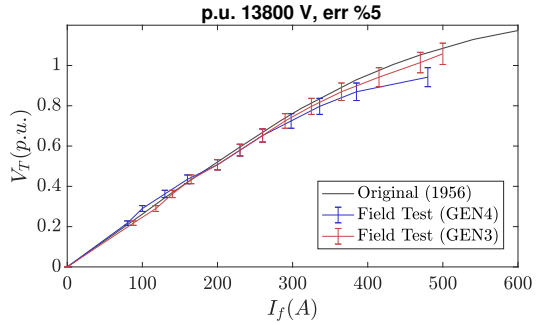

Fig. 4. Open circuit tests. Although GEN3 and GEN3 share the same design, the saturation characteristics are quite different.

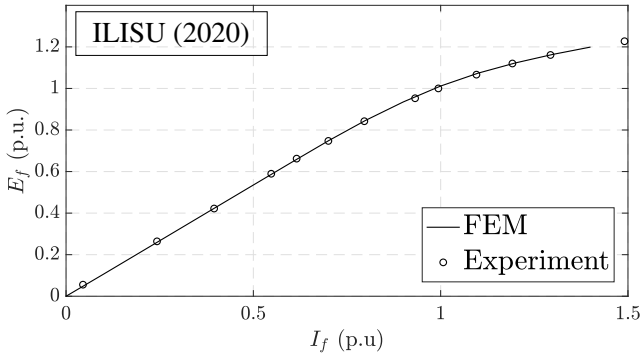

(a) The Ilisu generator.

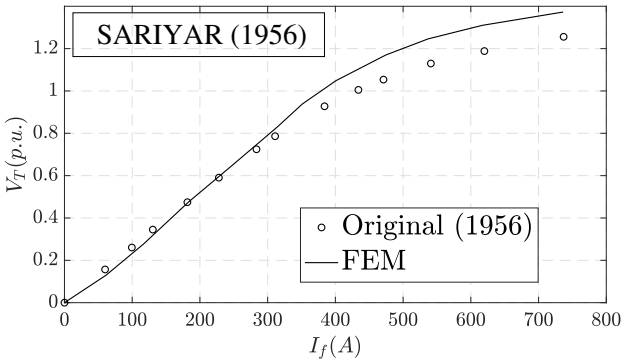

(b) The existing generator.

Fig. 5. Open circuit measurements, and FEA results.

kW to 160 kW. A return of investment table is made taking into account the widely used and locally accessible core materials. It is based on estimated core losses via an analytical model [10], and investment costs of various electrical steel types. The results are presented in Table II according to amortization duration in months. Although M400-50A is a common choice for generators due to its low cost, high silicon alternatives have a more economical impact.

2) Insulation Materials: A hydro generator's expected temperature rise is in the range of 60 °C, and this has a significant impact on the insulation's life. As a general rule, the life of the insulation material is reduced by half for every 10°C rise in temperature. While Class B insulations meet the requirement

TABLE II
TRADE-OFF TABLE.

		Reference			
		M270-50A	M310-50A	M350-50A	M400-50A
Selection	M270-50A	-	14	14	11
	M310-50A		-	15	10
	M350-50A			-	8
	M400-50A				-

* As an example, if M270-50A is **selected** with respect to M270-50A, the investment cost (since M270-50A is more expensive) redeems in 11 months (since M400-50A has more loss, electricity cost is used for amortization).

of temperature rise, for modern winding designs Class F insulations are used wherever possible [11]. The objective is the lowering the winding temperature as much as possible to secure a long lifetime.

C. Slot Number-Loading Selection

Although it is rare for refurbishment projects to modify the generator's slot number, doing so might have some important benefits. The machine's efficiency can improve if the designer modifies the electrical and magnetic loadings accordingly. Likewise, the machine's temperature distribution can be optimized. Since the design objective is utilizing Roebel bars, the number of the conductor in the slots is strictly two (for a double-layer winding). Thus, the slot number is directly affecting the electrical loading.

The machine properties can be significantly changed by the loading levels, so the selection process requires careful consideration. The initial values are chosen between 35-70 kA/mm. The optimum slot number is found by eliminating the poor ones first. The elimination is based on the following factors;

1) Winding scheme, ($k_w \geq 0.95$, cogging torque)
2) Manufacturing concerns, (avoiding core-splits, symmetric dovetail locations etc.)
3) Vibration profile (force harmonics, mechanical eigenfrequency analysis),
4) Short circuit ratio (SCR), field current limit.

Each factor is examined in the following subsections.

1) Winding Scheme: Fractional slot windings are a prevailing choice for large salient pole generators for the following reasons; first, they lessen the symmetry of the machine: which help to reduce cogging torque by diminishing zig-zag leakage reactance. Secondly, they reduce space harmonics; which can alleviate rotor surface losses. This article examines various winding scheme options using an algorithm that generates winding with $k_w \geq 0.95$.

2) Manufacturing Concerns: Laminations are cut with a tolerance because the hydrogenerators' stator diameters are frequently a few metres. This is important to secure stator ring's completeness. Then they are shifted axially which improves stator stiffness. The interlaminar clearance distance is shown in Fig. 6. If the laminations are not shifted axially, the clearance distance splits core into several pieces. This

introduces a serious mechanical vibration induced due to air-gaps. Numerous case studies and reports produced by the industrial partner demonstrate the negative consequences of core splits.

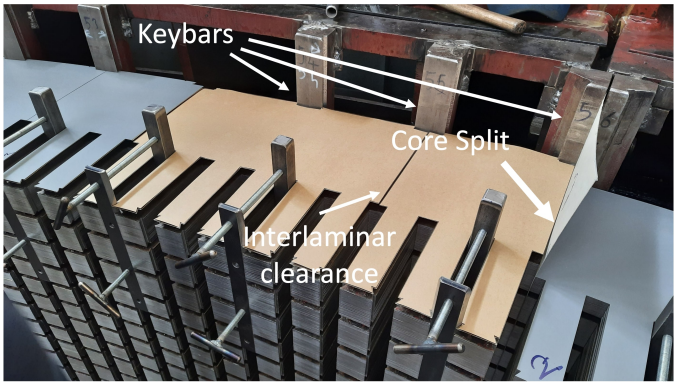

Fig. 6. Core split and interlamination clearance distance.

Simply shifting the laminations do not resolve this issue. Dovetails should be aligned with key bars. Moreover, the angle between key bars should not be a floating number since the alignment is another challenge for these large-diameters machines. Thus these concerns eliminate most of the slot number options.

The resultant slot number options are demonstrated in Table III. It should be noted that in order to have a slot number suitable for production not only θ_K should be an integer, but also Q_L/Q_K is forced to integer too. For example, when $Q = 324$, $N_L = 18$, $Q_L = 18$, $Q_K = 4$, and $N_K = 72$, θ_K is equal to 6°. However, since Q_L/Q_K is not an integer when the shifting is applied, laminations are not aligned considering key bar locations.

TABLE III
MECHANICAL COMPARISON OF DIFFERENT CANDIDATES.

Q	N_L	Q_L	Q_K	N_K	θ_K
240	30	8	4	60	6
270	18	15	3	90	4
288	36	8	4	72	5
300	30	10	5	60	6

Q : slot number, N_L : number of piece for one stack, Q_L : the slot number in one lamination piece, Q_K : slots per keybar, N_K : the number of keybars, θ_K : angle (°) between keybars.

3) Vibration Profile: Radial air-gap magnetic flux density does not produce power-producing torque. Instead, it generates radially oriented force waves. If the mechanical eigenfrequencies of the stator frame and the harmonic components of these waves overlap, extra care must be taken.

Large generators (>10 m diameter) might involve modes with high node numbers (N_m) larger than 20 [12]. The machine in this study can be considered as a medium-sized machine; the expected node numbers are between 10-20. A finite element (FE) model is constructed for eigenfrequency analysis. Laminations, finger plates, windings, spacers (ventilation ducts), and stator frames are included in the model. The first mode of vibration at 92.19 Hz with N_m is 12. This is the most hazardous mode since it is in the vicinity of the power frequency 100 Hz. Although there is a list of analytical eigenfrequency models in the literature [13]–[15], they are based on cylindrical shape assumption. They are validated mostly with smaller machines, and the interaction between the stator and core frame is more complex in large electrical machines [16], [17].

Hydro-generators are more susceptible to stress waves originating from armature MMF subharmonics. The reason is these machines have a high number of poles; the space harmonics of resultant airgap MMF have large wave numbers. They cannot excite dangerous stator modes. Traxler-Samek *et. al.* observed such an event [12]; 24^{th} node vibration at power frequency (in an unacceptable limit, 7 mm/s) supplied by stator-stator MMF interaction in a 112 MVA machine. Thus it is crucial to know the possible radial force spectrum for each winding design candidate. This feature is utilized as a deal-breaker; if there is any significant concern about the vibration profile the design is omitted.

D. Sizing

Short circuit ratio (SCR), is a metric for assessing generator stability. It is inversely proportional to the machine's direct-axis inductance, X_d. Greater than 1.1 is the expected value for a large salient pole generator; anything above that results in a size increase. Larger SCR requires less inductance which eventually results in a wider air-gap. More field current is required to achieve the necessary air-gap flux for the target voltage level. Due to additional rotor losses, this could cause the rotor geometry to grow in size and reduce efficiency. As a result, the majority of salient-pole generators have SCR values of 1.1. In order to have SCR equal to 1.1, the air-gap clearance is subsequently changed for each design candidate. To avoid the field exciter current limit and take into account thermal factors, the necessary field currents for the rated operation are also evaluated.

E. Loss Distribution

After the elimination process, the remaining machines should be quantitatively compared. This can be done with total electromagnetic loss calculation. However, this may lead to undesired results. The distribution of these losses is also crucial; for example, the peak temperature of the winding ($\hat{T}_w$) should be considered for insulation lifespan. It should be noted that the loss distribution can be altered by changing stator geometry. Nevertheless, this analysis made it first with different slot numbers in which tooth to slot width ratio is taken constant.

1) Core Loss: Core loss is calculated via the methodology presented in [10]. Formulas are developed to estimate the hysteresis and eddy current losses in the stator teeth and yoke. The induction waveform differences are taken into account in that regard. Minor loop correction factors are added to enrich

TABLE IV
DESIGN TABLE.

	Type	SCR	N	EL (kA/m)	ML (T)	g (mm)[1]	P_{loss}(kW)[2]	Vibration[3]	B_t[5]	M. Feasible?	Comment
240	Diamond	1.03	100	57.32	0.90	18.0	421	✓	1.54	✓	Reference
240	Roebel	1.10	80	46.06	1.20	4.3	486	✓	1.99	✓	B_t is the DB.
270	Roebel	1.10	90	51.69	1.03	12.1	404	✓	1.82	✓	B_t is the DB.
288	Roebel	1.10	96	55.06	0.92	15.8	405	×	1.77	✓	T_c is the DB.
300	Roebel	1.10	100	57.32	0.90	17.7	399	✓	1.72	✓	-
324	Roebel	1.10	108	61.83	0.82	22.2	406	✓	1.67	×	M. is the DB.

[1] g is calculated by making SCR equal to 1.1.
[2] Includes electromagnetic losses; includes armature copper loss, field copper loss, damper loss and core loss.
[3] It considers natural frequency modes of the stator at double frequency stress wave originated from subharmonics of armature MMF.
[5] No-load rated voltage operation.

the model whereas the effect of the rotational field [18] is ignored. The objective is the lightning-fast model.

2) Copper Loss: Since the 360° transposition is applied to the armature winding, the circulating current can be neglected. 75 C° is chosen as the operation temperature, and the conductivity values are arranged accordingly. The fill factor is calculated considering strand insulation, ground-wall insulation, fillers, and wedges.

Results are finalized in Table IV. $Q = 240$ is eliminated for its non-realistic g. $Q = 270$ has large B_t, and its one of the MMF subharmonic interactions with the machine eigenfrequency. $Q = 288$ has large cogging torque since it is integer slot winding. Moreover, $Q = 324$ has manufacturing issues as aforementioned before. Thus, Q is selected as 300.

III. STATOR DESIGN AND RESULTS

After choosing a Q, the stator geometry is optimized from an electromagnetic and thermal standpoint. A parametric sweep is used to calculate the slot geometry while aiming for an advantageous loss distribution. Without altering the equivalent magnetic length, cooling ducts are optimized. In order to determine lamination stack thicknesses, a computational fluid dynamics (CFD) model is built.

A. Electromagnetic Design

Since the rotor and the stator frame are kept without change, the design parameters are g, slot width, slot height, number of ventilation ducts, and duct thickness. Duct geometry is optimized such that the equivalent magnetic length is constant. g is determined such that SCR is equal to 1.1.

B. Thermal Design

Compared to more recent generators, older ones have larger ventilation ducts. Having more ducts with less thickness can be practical. This increases the cooling region, without affecting the axial-magnetic length. Additionally, the airflow within these ducts might vary. This creates an irregular temperature distribution. Thus, a CFD model is constructed to correctly model irregularities in air flow. The models are listed as follows;

1) **Original**: Stack geometry and loss values is belong the original machine. Vent thickness (w_{duct}) is 8.5 mm, and it is uniform.
2) **D1**: Stack geometry belongs to the original machine. The loss values are updated and considered the new machine design. This value is used for all analyses after this point,
3) **D2**: w_{duct} is decreased to 6.5 mm. w_{stack} is uniform across to axial length,
4) **D3**: Thinner bottom lamination stacks are used since the hot spot is placed at the bottom side,
5) **D4**: w_{stack} values are adjusted to have optimum air flow and temperature distribution.

The $\hat{T}_w$, and the average copper temperature (T_w) are listed in Fig. 7. By optimizing the stack geometry, an 11 $°C$ decrease in T_w is obtained. This is a significant reduction considering the insulation lifetime. The temperature distributions for the original machine and the designed machine are shown in Fig. 8.

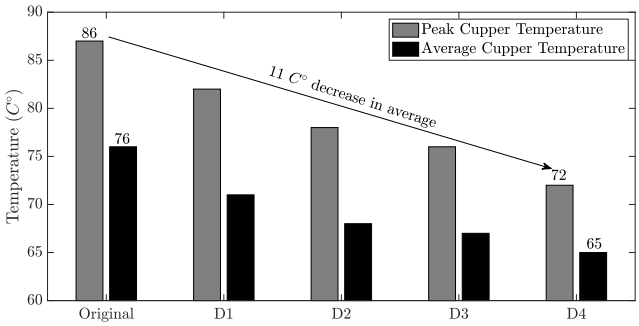

Fig. 7. Peak and average copper temperatures at stator.

C. Result

The resultant machine and its comparison with the existing generator is shown in Table V. The efficiency of the machine is increased by 0.21%, which corresponds to 100 kW reduction in losses. Such reduction decreases the $\hat{T}_w$ by 3 $°C$, and reduces the T_w by 6 $°C$. $\hat{T}_w$ is further decreased by a series of design steps.

IV. CONCLUSION

This study employs an electrical machine design methodology where the primary focus is on alternating windings. While maintaining the stator frame, and the rotor, Q is increased from

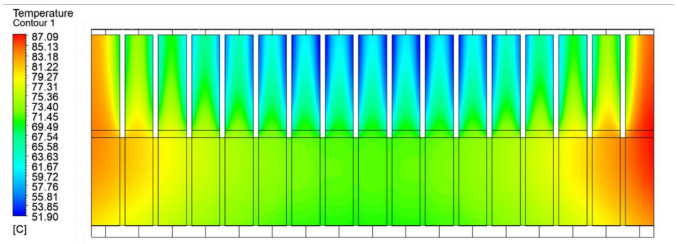

(a) Original design.

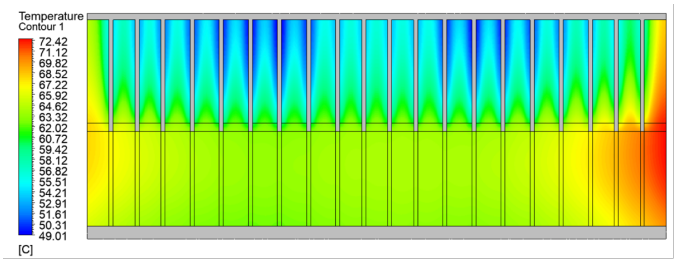

(b) The new design.

Fig. 8. Temperature distributions.

TABLE V
THE COMPARISON BETWEEN THE DESIGNED AND CURRENT MACHINES.

	Current	New
Slot Number (mm)	240	300
Slot Width (mm)	25.2	22
Air gap (mm)	18.5	18
Number of ventilation duct	16	20
Duct thickness (mm)	8.5	6.5
Winding Type	Diamond	Roebel
Stator Copper Loss (kW)	101	99
Core Loss (kW)	220	158
Field Copper Loss (kW)	87.5	58
Full load efficiency (%)	97.99	98.20
Peak Temperature (C°)	86	72
SCR	1.02	1.10
Peak short-circuit current (kA)	11.6	11.7

240 to 300. The methodology is deductive, possible design candidates are filtered through several considerations. These are;

1) Vibration problems: high cogging torque ($Q = 288$), sub-harmonic interaction ($Q = 270$).
2) Manufacturability: poor keybar location ($Q = 252$), split core prevention ($Q = 324$).
3) SCR, and field exciter limit: non-realistic air-gap ($Q = 240$).

After the Q selection, an optimum slot geometry is obtained considering the loss distribution. The stacking structure is optimized by doing CFD analyses. An 11 $^{\circ}C$ decrease in T_w. This article promises a design methodology to designers who work on large-generator refurbishment projects.

REFERENCES

[1] M. M. Znidarich, "Upgrading and uprating of hydro generators: An australian perspective," *Australian Journal of Electrical and Electronics Engineering*, vol. 10, no. 1, pp. 75–84, 2013. [Online]. Available: https://www.tandfonline.com/doi/abs/10.7158/1448837X.2013.11464357

[2] ——, "Hydro generator stator cores part 1 - constructional features and core losses," in *2008 Australasian Universities Power Engineering Conference*, 2008, pp. 1–8.

[3] ——, "Hydro generator stator cores part 2 - core losses, degradation mechanisms, testing and specification," in *2008 Australasian Universities Power Engineering Conference*, 2008, pp. 1–9.

[4] M. Znidarich, "Hydro generator high voltage stator windings: Part 1 – essential characteristics and degradation mechanisms," *Australian Journal of Electrical and Electronics Engineering*, vol. 5, no. 1, pp. 1–17, 2008. [Online]. Available: https://doi.org/10.1080/1448837X.2008.11464196

[5] ——, "Hydro generator high voltage stator windings: Part 2 - design for reduced copper losses and elimination of harmonics," *Australian Journal of Electrical and Electronics Engineering*, vol. 5, no. 2, pp. 119–135, 2009. [Online]. Available: https://doi.org/10.1080/1448837X.2009.11464206

[6] ——, "Hydro generator high voltage stator windings: Part 3 - stator winding slot support systems," *Australian Journal of Electrical and Electronics Engineering*, vol. 6, no. 1, pp. 1–10, 2009. [Online]. Available: https://doi.org/10.1080/1448837X.2009.11464221

[7] ——, "Hydro generator high voltage stator windings: Part 4 – type and routine production testing," *Australian Journal of Electrical and Electronics Engineering*, vol. 6, no. 2, pp. 93–108, 2009. [Online]. Available: https://doi.org/10.1080/1448837X.2009.11464229

[8] "Ieee guide for test procedures for synchronous machines including acceptance and performance testing and parameter determination for dynamic analysis," *IEEE Std 115-2019 (Revision of IEEE Std 115-2009)*, pp. 1–246, 2020.

[9] J. C. Akiror, P. Pillay, and A. Merkhouf, "Challenges in modeling of large synchronous machines," *IEEE Transactions on Industry Applications*, vol. 54, no. 2, pp. 1652–1662, 2018.

[10] F. Deng, "An improved iron loss estimation for permanent magnet brushless machines," *IEEE Transactions on Energy Conversion*, vol. 14, no. 4, pp. 1391–1395, 1999.

[11] M. Znidarich, "Hydro generator high voltage stator windings: Part 1 – essential characteristics and degradation mechanisms," *Australian Journal of Electrical and Electronics Engineering*, vol. 5, no. 1, pp. 1–17, 2008. [Online]. Available: https://doi.org/10.1080/1448837X.2008.11464196

[12] G. Traxler-Samek, T. Lugand, and M. Uemori, "Vibrational forces in salient pole synchronous machines considering tooth ripple effects," *IEEE Transactions on Industrial Electronics*, vol. 59, no. 5, pp. 2258–2266, 2012.

[13] R. Girgis, "Method for accurate determination of resonant frequencies and vibration behaviour of stators of electrical machines," *IEE Proceedings B (Electric Power Applications)*, vol. 128, pp. 1–11(10), January 1981. [Online]. Available: https://digital-library.theiet.org/content/journals/10.1049/ip-b.1981.0001

[14] S. Verma, "Experimental verification of resonant frequencies and vibration behaviour of stators of electrical machines. part 1: Models, experimental procedure and apparatus," *IEE Proceedings B (Electric Power Applications)*, vol. 128, pp. 12–21(9), January 1981. [Online]. Available: https://digital-library.theiet.org/content/journals/10.1049/ip-b.1981.0002

[15] ——, "Experimental verification of resonant frequencies and vibration behaviour of stators of electrical machines. part 2: Experimental investigations and results," *IEE Proceedings B (Electric Power Applications)*, vol. 128, pp. 22–32(10), January 1981. [Online]. Available: https://digital-library.theiet.org/content/journals/10.1049/ip-b.1981.0003

[16] J. Sobra and M. Byrtus, "Impact of electrical machine structural parts on its modal and vibration behavior," in *IECON 2019 - 45th Annual Conference of the IEEE Industrial Electronics Society*, vol. 1, 2019, pp. 1107–1113.

[17] A. de Barros, A. Galai, A. Ebrahimi, and B. Schwarz, "Practical modal analysis of a prototyped hydrogenerator," *Vibration*, vol. 4, no. 4, pp. 853–864, 2021. [Online]. Available: https://www.mdpi.com/2571-631X/4/4/48

[18] M. Ranlof, A. Wolfbrandt, J. Lidenholm, and U. Lundin, "Core loss prediction in large hydropower generators: Influence of rotational fields," *IEEE Transactions on Magnetics*, vol. 45, no. 8, pp. 3200–3206, 2009.